Regional Variability of the Arctic Heat Budget in Fall and Winter*

JENNIFER MILETTA ADAMS AND NICHOLAS A. BOND

Joint Institute for the Study of the Atmosphere and Ocean, University of Washington, Seattle, Washington

JAMES E. OVERLAND

NOAA/Pacific Marine Environmental Laboratory, Seattle, Washington

(Manuscript received 7 June 1999, in final form 29 November 1999)

ABSTRACT

In the Arctic atmosphere, the fall cooling cycle involves the evolution of the zonally symmetric circulation in late summer into the asymmetric flow of winter. This paper uses historical reanalysis data to document how the dominant components of the Arctic heat budget influence the summer–winter transition. The spatial variability of 20-yr climatologies of 700-mb temperature and geopotential height, the net surface flux, and the horizontal convergence of eddy sensible heat fluxes are examined for September through February.

The development of the zonal asymmetries in the temperature and geopotential height fields in the Arctic is linked to the land–water–ice distribution that regulates the surface fluxes and the baroclinic zones in the hemispheric circulation, which lead to regional heating/cooling by the transient and standing eddies. These eddies serve to transport the heat energy gained via the surface fluxes over the North Atlantic and North Pacific to the continental and ice-covered regions of the central Arctic, where the net surface flux is small. The transient eddies are especially important in the Atlantic and Eurasian sectors of the Arctic, while the standing eddies play the larger role in the heat budget on the Pacific side of the Arctic in early to mid-winter.

The Arctic oscillation (AO) has a small effect on the basinwide pattern of heating and cooling by the eddy circulations, but on smaller spatial scales there are isolated regions where the AO influences the Arctic heat budget.

1. Introduction

Local atmospheric energy budgets are the sum of radiative, sensible, and latent heating balanced against the transport of energy by atmospheric motions. Each of these components varies greatly according to geographic location and season. In the polar regions, the seasonal cycle of solar heating is particularly extreme; as insolation decreases to zero, the poleward transport of energy and outgoing longwave radiation become the dominant components of the energy budget. At high latitudes, the poleward energy transport is accomplished primarily by the standing and transient eddy circulations.

Information about the scales of space and time on which the atmospheric eddy fluxes occur is of value for understanding the mechanisms of the Arctic climate and its short- and long-term variability. The decomposition of energy transport reveals a signature of high-latitude atmospheric dynamics that can be used to evaluate GCM simulations (Genthon and Krinner 1998). Unfortunately, many of the papers that address eddy fluxes at high latitudes present zonal mean statistics (e.g., van Loon and Williams 1980; Holopainen and Fortelius 1986; Michaud and Derome 1991; Kann et al. 1994; Keith 1995) or averages over the area poleward of 70° (e.g., Nakamura and Oort 1988; Genthon and Krinner 1998). It is important to study polar climate variables on regional spatial scales in order to bridge the gap between the point measurements of the physical processes influencing local ocean–ice–atmosphere feedbacks and the coupled general circulation models that are predicting the role of the Arctic and Antarctic in the global environment.

Previous work by the authors has diagnosed the regional variability of moist static energy flux in the Arctic (Overland et al. 1996) and examined the relationship between temperature and circulation patterns in the Arctic (Overland et al. 1997). Both papers identify important regional differences in the winter climate of the

* Joint Institute for the Study of the Atmosphere and Ocean Contribution Number 685 and Pacific Marine Environmental Laboratory Contribution Number 2099.

Corresponding author address: Jennifer Miletta Adams, Code 913, NASA GSFC, Greenbelt, MD 20771.
E-mail: adams@janus.gsfc.nasa.gov

Arctic in terms of the thermal fields and their dynamical forcing. This paper seeks to build on those results by asking the question: ''When and how are the asymmetries of the Arctic winter climate established?''

Our first step is to diagnose the spatial and temporal variability of tropospheric temperature and circulation patterns in the Arctic during the fall cooling period, when the zonally symmetric flow of late summer evolves into the asymmetric flow of midwinter. The fall cooling period is a part of the annual cycle that is seldom discussed in the Arctic literature. Previous studies on similar topics generally present January climatologies or November–March averages (e.g., Lau 1979; Higuchi et al. 1991), and discussions of the seasonal cycle are often reduced to a comparison of summer and winter conditions (e.g., Michaud and Derome 1991; Mock et al. 1998).

Our next step is to examine the spatial and temporal variability of the dominant components of the Arctic heat budget during the fall cooling period. In particular, we consider the sum of the net radiative, sensible, and latent heat fluxes at the surface, and the vertical integral of convergence of heat flux by transient and standing eddies. We focus on how these parameters relate to the tropospheric circulation in the Northern Hemisphere, with an emphasis on the role played by eddy circulations in establishing the regional temperature differences in the Arctic.

We seek to understand the aspects of the interaction between the Arctic and hemispheric circulation that are relevant to the Arctic during the fall cooling cycle. We hypothesize that the interactions between the midlatitude tropospheric flow and the surface forcing in the Arctic are responsible for the regional variations in the Arctic winter climate.

2. Data sources

Studying the spatial variability of the many components of Arctic climate has become easier now that the available gridded atmospheric analyses have been retooled for diagnosing climate and climate variability. The reanalysis efforts led by the National Aeronautics and Space Administration, National Centers for Environmental Prediction–National Center for Atmospheric Research (NCEP–NCAR), and the European Centre for Medium-Range Weather Forecasting (Schubert et al. 1993; Kalnay et al. 1996; Gibson et al. 1997) have produced a long-term record of global gridded atmospheric variables that are constrained by observational data but lack the artificial climate signals induced by ongoing changes to the numerical prediction models and analysis systems. The models used for the reanalysis also provide previously unavailable geophysical variables (e.g., cloud information, precipitation, and radiative fluxes) that are based in a physically consistent framework. The reanalyses are particularly valuable in the Arctic, where observational data are not quite adequate for regional studies, but are sufficient to constrain the data assimilation system so that the gridded reanalyses can be used to characterize the Arctic atmosphere.

The reanalysis data used in this study are from NCEP–NCAR (Kalnay et al. 1996). Almost all of the parameters discussed are derived from fundamental meteorological variables (e.g., wind, temperature, and geopotential height) that are strongly influenced by the assimilated observations and accurately represent the Arctic atmosphere, especially at upper levels (Overland et al. 1997). The radiative, sensible, and latent heat fluxes are model-predicted variables and may be less reliable in representing the real atmosphere.

Serreze et al. (1998) and Walsh and Chapman (1998) compared reanalysis data to independent observations in the Arctic and their results give us more confidence in the reanalysis surface flux data used in this study. Serreze et al. (1998) compiled a monthly climatology of downwelling shortwave radiation for the Arctic and observed that the NCEP reanalysis correctly depicts the observed spatial patterns of the surface fluxes but the magnitudes are too high. This is more of a problem in the summer months. Net shortwave fluxes in the Arctic are small in September and October and negligible from November to February. Walsh and Chapman (1998) have also compared reanalysis data to surface-based observations in the Arctic and concluded that the reanalysis captures the seasonality and actual values of surface air temperatures, a critical element of the parameterization for sensible heat flux. The net longwave fluxes in the NCEP reanalysis compared well with the observations as well as satellite-based fluxes derived by Schweiger and Key (1994). Sea ice extent is an observational dataset that is assimilated into the reanalysis; however, leads or cracks in the Arctic sea ice are not explicitly resolved or parameterized, so the latent heat flux over sea ice is effectively zero.

NCEP has acknowledged a problem with the reanalysis humidity fields (Kalnay et al. 1998; see also online at http://wesley.wwb.noaa.gov/spurious_h2o.html). A diffusion approximation led to a spurious moisture source/sink that is manifest as quasi-stationary small-scale features in the moisture-related variables. This problem is particularly noticeable at high latitudes in winter. Long time averaging helps to smooth out these features.

The reanalysis data are available from NCEP online at http://wesley.wwb.noaa.gov/reanlysis.html. Additional reanalysis data were provided by the National Oceanic and Atmospheric Administration–Cooperative Institute for Research in Environmental Sciences Climate Diagnostics Center at http://www.cdc.noaa.gov. Surface station data were provided by the Polar Exchange at the Sea Surface project at the University of Washington.

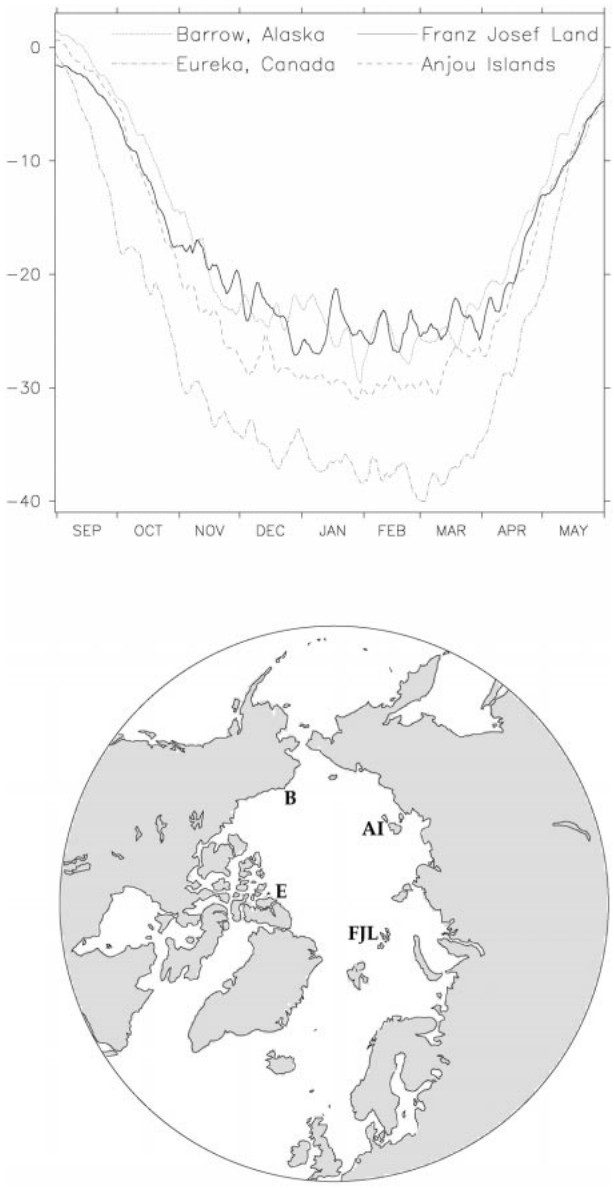

FIG. 1. (top) Daily surface air temperatures at four land stations around the perimeter of the Arctic averaged over 17 cold seasons (1979–95) and smoothed with a 5-day running mean. (bottom) The locations of the stations. Franz Josef Land (solid line) is at 80.6°N, 58°E; the Anjou Islands (dashed line) is at 76°N, 138°E; Barrow, Alaska (dotted line) is at 71.3°N, 156°W; and Eureka, Canada (dot–dashed line) is at 80°N, 86°W.

3. Meteorological variables

a. Surface air temperature

Figure 1 contains time series of daily surface air temperatures averaged over seventeen cold seasons (1979–95) at four land stations around the perimeter of the Arctic. These four stations (Eureka, Barrow, the Anjou Islands, and Franz Josef Land) are distributed among the four quadrants of the Arctic, roughly divided into North American/Eurasian and Atlantic/Pacific sectors. The map at the bottom of Fig. 1 shows the approximate locations of the stations.

The onset of cooling in the fall occurs earliest in the Canadian Archipelago (Eureka) and the coldest temperatures are maintained in this region throughout the winter. Surface temperatures at the other three stations start to cool later in September and cool more gradually. Temperatures at these stations are 10°–15°C warmer than Eureka from November to March. As winter progresses, the Anjou Islands are consistently colder than Barrow and Franz Josef Land; the surface temperature climatology might be closer to Eureka's if it were not for the 4°-latitude difference between these two stations.

The examination of the temperatures at these four stations and others in the surrounding areas shows that surface temperatures during the fall and winter are generally colder in the central-North American and Asian sectors compared to the Atlantic and Pacific sectors. It will be shown in the following section that this temperature pattern extends from the surface deep into the troposphere, indicating that the surface conditions are strongly linked to the tropospheric flow.

The remainder of figures in this paper are 20-yr means covering the period 1979–98. The figures are all constructed in a similar fashion, containing three 2-month means for each variable: the September–October mean (fall), the November–December mean (early winter), and the January–February mean (mid winter). The map projections are polar stereographic and show the area poleward of 50°N.

b. Tropospheric temperature and circulation patterns

We use the 700-mb level to illustrate the tropospheric temperature and circulation patterns. Atmospheric parameters at this level reflect the large-scale circulation patterns of the upper troposphere, yet are also connected to the temperature patterns at the surface. The 700-mb level is high enough to avoid the influence of small-scale surface inhomogeneities yet low enough to capture the variability of Arctic synoptic weather systems, which tend to be shallower than their midlatitude counterparts.

Figure 2 contains the 2-month means of 700-mb temperatures. The extremely cold 700-mb temperatures observed over Greenland's high plateau are a manifestation of surface effects and are therefore excluded from this discussion. The spatial variability of the 700-mb temperatures is consistent with the surface temperature data shown in Fig. 1. Departures from zonal symmetry first appear in the western Arctic in fall (Fig. 2a). By early winter (Fig. 2b), the temperature field has evolved into a wavenumber-2 pattern; colder temperatures stretch from the Canadian Archipelago across the central Arctic and into eastern Siberia, whereas the ice-covered Barents and Kara Seas on the east side and the Beaufort and Chukchi Seas on the west side are slightly warmer. In midwinter (Fig. 2c), the polar vortex has become well

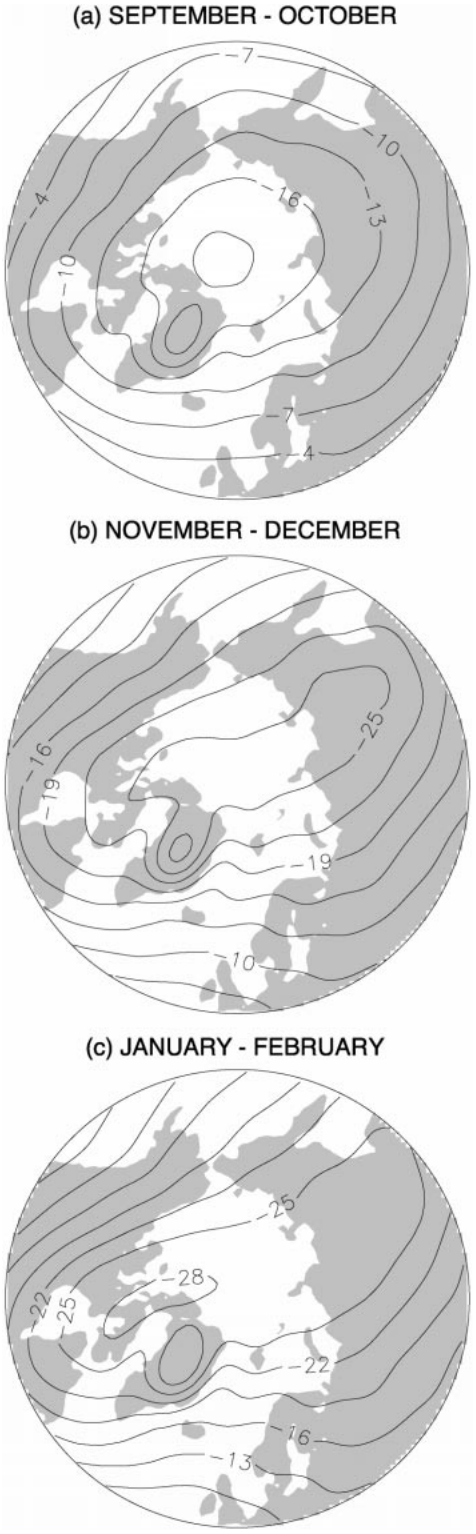

FIG. 2. Two-month means of 700-mb temperature for 1979–98. (a) Sep–Oct, (b) Nov–Dec, and (c) Jan–Feb. The contour interval is 3°C.

established in the western Arctic (Overland et al. 1997), and the coldest temperatures are over the Canadian Archipelago.

The 2-month mean 700-mb geopotential height fields are shown in Fig. 3. The height field in fall shows slight zonal asymmetries aligned with land–sea boundaries; heights are higher over the continents and lower over the Bering Sea and North Atlantic Ocean. As the cold season progresses, the height fields evolve into a pattern that persists throughout the late fall and winter: a broad trough forms over eastern Siberia and the Bering Sea as well as over northern Canada, while a moderate ridge extends from western North America into the central Arctic. The lowest heights are collocated with the coldest temperatures over the Canadian Archipelago.

The 700-mb temperature and height distributions indicate that the mean circulation at high latitudes in the Northern Hemisphere is, for the most part, equivalent barotropic; that is, the temperature and height contours are essentially parallel. A region of prominent exception extends from central Siberia to the Bering Sea during early to mid-winter. The broad trough in 700-mb heights over the eastern extremity of Siberia and the Bering Sea is eastward of the temperature trough over central Siberia. This offset implies persistent cold air temperature advection on the west side of the height trough and warm air advection on the east side of the height trough, along the coast of western North America. A zone of warm advection is also present across central Siberia.

4. The atmospheric heat budget

Local temperature changes are due to the effects of radiation, latent heating, sensible heat exchange with file surface and energy transport (Hartmann 1994). Each of these terms varies over a broad range of spatial and temporal scales, and their dominance of the local energy budget also varies by season and location.

In this study, we treat each 2.5° grid cell as an independent column, and calculate the net flux of energy at the surface as well as the energy that is advected in and out of the sides of each column. Our objective is not to completely close the atmospheric energy budget for each column in the Arctic; rather, we focus on the broad regional distribution of the few dominant components of the energy budget and examine their relationship to the tropospheric temperature and circulation patterns.

a. Net surface flux

An important source of heat in the Arctic in fall and winter is the flux from the surface. We estimate the total surface flux as the sum of the net longwave flux (NLW, up–down), the net shortwave flux (NSW, down–up), the sensible heat flux (SH) and the latent heat flux (LH):

$$Q_{\text{net}} = \text{NLW} - \text{NSW} + \text{SH} + \text{LH}. \qquad (1)$$

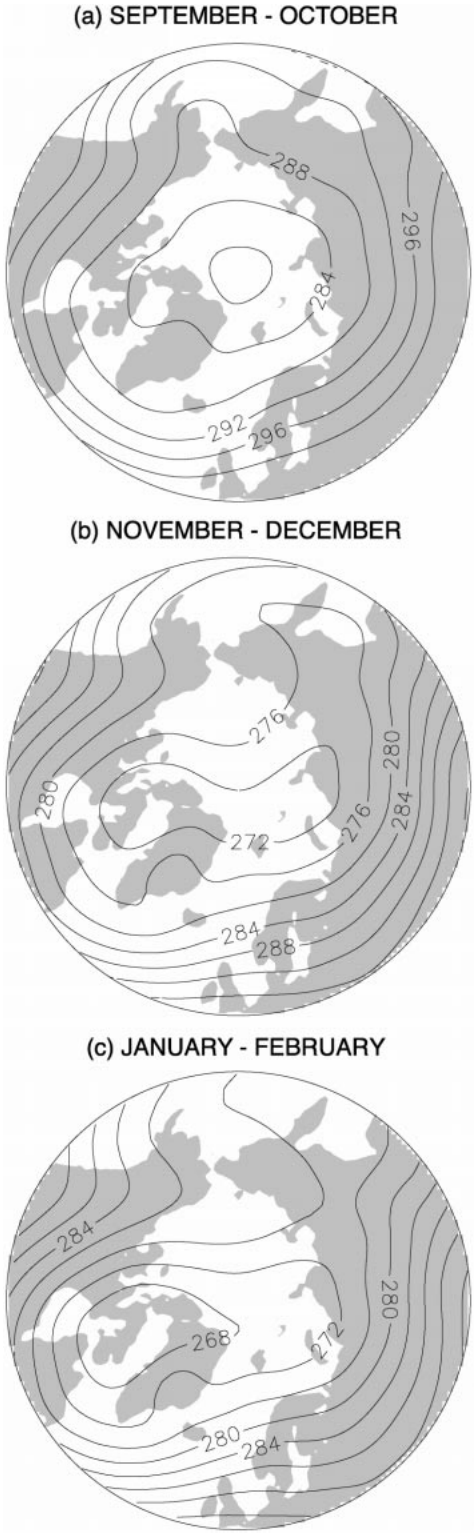

FIG. 3. Two-month means of 700-mb height for 1979–98; (a) Sep–Oct, (b) Nov–Dec, and (c) Jan–Feb. Heights are plotted in dekameters.

The net flux at the surface (Q_{net}) is positive upward and represents heat transferred to the atmosphere from the surface. Two-month mean plots of Q_{net} are shown in Fig. 4; the darker the gray shade, the larger the net surface flux. Maximum values are located over the open water of the high-latitude oceans in the winter months. Net surface fluxes as high as 400 W m^{-2} occur in the Labrador Sea and near the ice edge around Spitsbergen. These regions where the net surface flux is very large do not precisely correspond to the regions of warmer tropospheric temperatures. The heat energy from the net surface flux is redistributed horizontally around the Arctic by the eddy circulations. The net surface flux is not a major contributor to the atmospheric heat budget over the continents or the ice-covered central Arctic.

b. Eddy heat flux convergence

Meridional transport of energy by the atmosphere may be divided into contributions from the mean meridional circulation (MMC) and the eddy or wave motions that are superimposed on the zonal mean flow (Hartmann 1994). Eddy energy transport is more important at mid- and high latitudes, whereas the MMC is dominant in the Tropics; the MMC is not well-defined in the high Arctic. Meridional energy transport may be further partitioned by separating out the standing and transient eddy components as well as the individual terms of moist static energy (i.e., potential energy, latent heat, and sensible heat). Eddy transport of potential energy is small, eddy transport of latent heat peaks in the subtropics, and eddy transport of sensible heat peaks around 50° where it constitutes about 80% of the total poleward energy flux (Hartmann 1994). The problems with the NCEP moisture fields discussed in section 2 and the fact that the moisture fluxes in the Arctic are very small in fall and winter [an equivalent heating O(10 W m^{-2})] led us to exclude the moisture fluxes from this analysis. We therefore limit our discussion to the horizontal convergence (and divergence) of the eddy sensible heat fluxes that are the dominant contributors to the total meridional energy transport in the Arctic and are primarily responsible for the local temperature tendencies.

1) TRANSIENT EDDIES

Using daily values of temperature and horizontal wind vector components, we calculated the vertical integral of the convergence of heat flux by transient eddies using the following expression:

$$-\frac{c_p}{g}\int\left[\frac{\partial}{\partial x}(u'T') + \frac{\partial}{\partial y}(v'T')\right]dp, \qquad (2)$$

where the primes indicate a departure from a monthly mean. The c_p/g factor converts the units to W m^{-2}, and

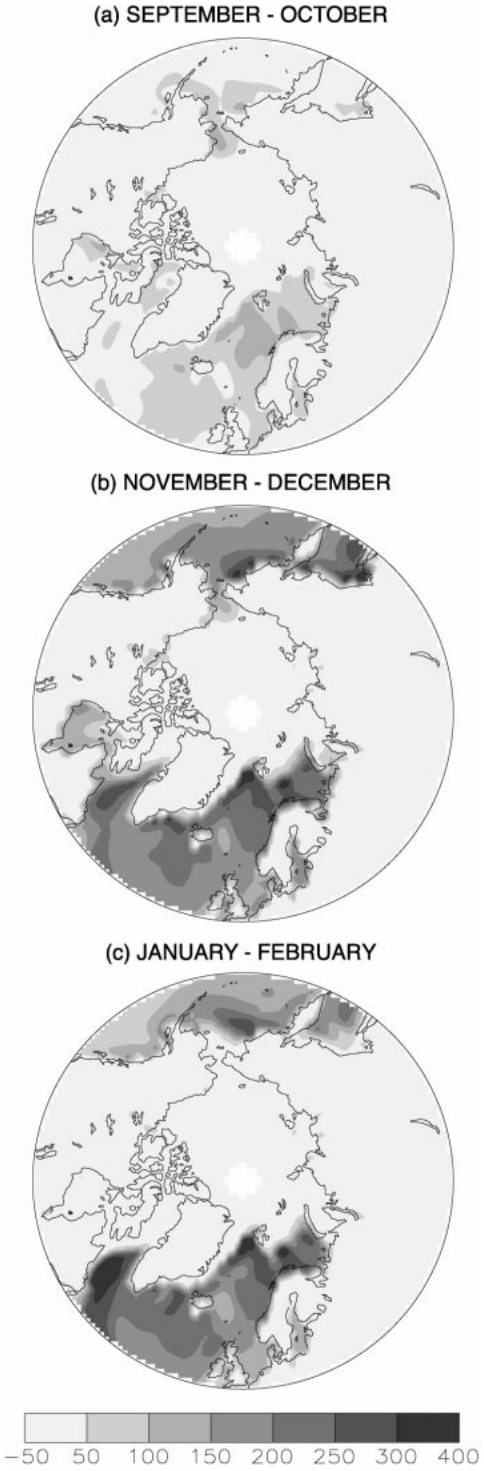

FIG. 4. Two-month means of net surface flux for 1979–98 (W m^{-2}): (a) Sep–Oct, (b) Nov–Dec, and (c) Jan–Feb.

the minus sign in front of the integral allows positive values to indicate convergence, or heating of the column, and negative values to indicate divergence, or cooling of the column. The vertical integration is calculated from the 1000-mb level to the top of the atmosphere (10 mb).

Daily values of the vertically integrated transient eddy heat flux convergence were averaged to create the 2-month means shown in Fig. 5. Negative or divergent values are drawn with dotted lines, positive or convergent values are drawn with solid lines, and the contour interval is 25 W m^{-2}.

The transient eddies largely heat the Arctic, but in a manner that varies seasonally. In fall, heating occurs in a relatively broad, diffuse pattern at a typical rate of 25–40 W m^{-2}. As winter progresses, this heating becomes more concentrated in the western Arctic over northern Canada and, to a lesser extent, over northern Russia and Siberia. The heating due to transient eddies peaks during midwinter with values around 200 W m^{-2}. This seasonal increase in localized heating is accompanied by the development of significant cooling in two regions: one covers western North America and Alaska, spreading across the Bering Sea as winter progresses, the other extends from the North Atlantic over the Greenland–Iceland–Norwegian (GIN) Seas and into the Barents Sea. Serreze et al. (1993) show that synoptic activity is greatest in the eastern/Atlantic quadrant of the Arctic. The heat flux divergence maximum in this region is ~125 W m^{-2} in midwinter.

The net effect of the transient eddies is to take the heat gained via the surface energy fluxes from the North Atlantic and North Pacific Oceans and redistribute it downstream and poleward into the central Arctic. This heating of the central Arctic and high-latitude land masses counteracts the net loss of heat due to radiation. The regions of maximum heating (cooling) by the transient eddies are collocated with the relatively cold (warm) regions in the 700-mb temperature field, although the heating by the transient eddies is distributed over a smaller area in the western Arctic than in the eastern Arctic.

2) STANDING EDDIES

The regions of systematic temperature advection evident in Figs. 2 and 3 and discussed at the end of section 3b suggest that the standing eddy circulations are important to the Arctic heat budget. Using daily values of temperature and horizontal wind vector components, we calculated the vertical integral of the convergence of heat flux by standing eddies using the following expression:

$$-\frac{c_p}{g}\int\left[\frac{\partial}{\partial x}(\overline{u}^*\overline{T}^*)+\frac{\partial}{\partial y}(\overline{v}^*\overline{T}^*)\right]dp, \qquad (3)$$

where the overbar indicates a monthly mean and the asterisk indicates a departure from a zonal mean. As with the transient eddy flux convergence, units are watts per meter squared, positive values indicate convergence/heating, and negative values indicate divergence/cooling. The vertical integration of the standing

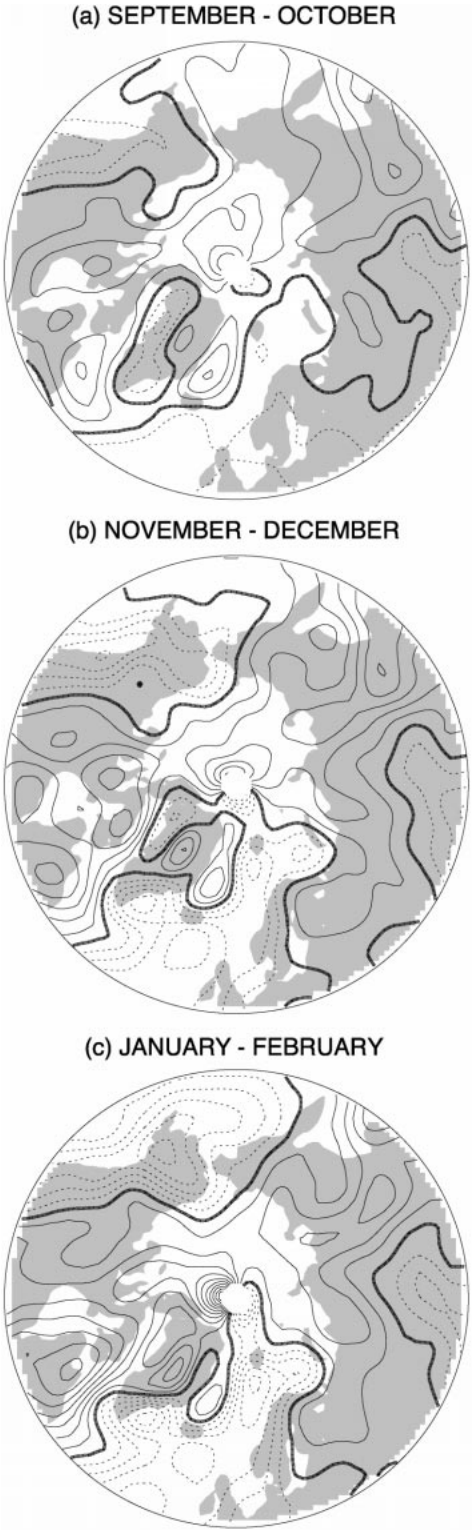

FIG. 5. Two-month means of the vertically integrated convergence of heat flux by transient eddies for 1979–98: (a) Sep–Oct, (b) Nov–Dec, and (c) Jan–Feb. The contour interval is 25 W m^{-2}. Negative values, drawn with dotted contours, represent heat flux divergence or a cooling of the column; positive values, drawn with solid lines, represent heat flux convergence or a warming of the column. The thick solid line is the zero contour.

eddy heat flux is calculated from the 700-mb level to the top of the atmosphere to avoid the noisy spatial variability close to the surface caused by local topography.

Monthly values of the vertically integrated standing eddy heat flux convergence were averaged to create the 2-month means shown in Fig. 6. The standing eddy flux convergence is not an important component of the heat budget in fall (Fig. 6a). By early winter (Fig. 6b), the standing eddy flux convergence acts to heat most of the Arctic, with especially large values over far eastern Siberia. By midwinter (Fig. 6c), the standing eddy flux convergence is the dominant component of the heat budget in eastern Siberia, northern Canada, and Greenland. Note that the standing eddy flux convergence is near zero in the European and central Siberian sectors of the Arctic.

The warming over Greenland is associated with the transport of relatively cold surface-cooled air off the Greenland plateau, and its replacement by warmer air from the south. A portion of the cold air flowing off Greenland appears to be entrained into the polar vortex over the Canadian Archipelago, thereby reinforcing its temperature signature, as evidenced by the area of cooling in Fig. 6c.

5. Discussion

A large body of work has been dedicated to documenting and understanding the relationships between the stationary and transient eddies and the mean hemispheric flow (e.g., Hoskins and Pearce 1983, and references therein). Here we focus on the elements of that broad subject that are relevant to the Arctic climate during the fall cooling cycle. The climate in the Arctic is generally ascribed to the extreme seasonal cycle of radiation, the surface characteristics (i.e., land–water–ice distributions), and the seasonal variations of the hemispheric circulation. The key aspects of the latter pertain to the migration and strengthening of the tropospheric jet stream and the role of the eddies in transporting energy poleward.

In September and October, the mean flow poleward of 50°N is essentially zonally symmetric and equivalent barotropic, resulting in standing eddy flux convergences near zero. However, the synoptic-scale variability at high latitudes is substantial, so that transient eddy flux convergence produces heating in the Arctic of approximately 30 W m^{-2}, a significant value when compared with the two other primary terms in the heat budget: the surface heat flux ($\sim$50 W m^{-2}) and radiational cooling ($\sim$100 W m^{-2}). The absolute values of the transient eddy flux convergence continue to increase as winter progresses (Fig. 5).

As fall cooling continues, the mean meridional temperature gradient sharpens and shifts equatorward. The resulting spin up of the hemispheric circulation increases the zonal mean available potential energy, encour-

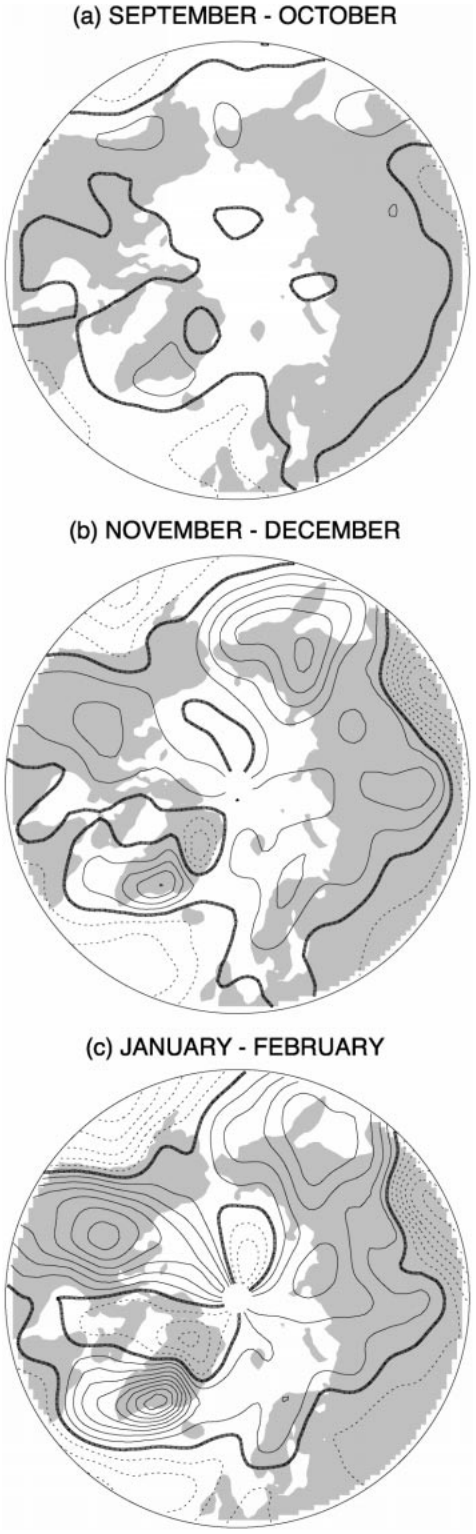

FIG. 6. Two-month means of the vertically integrated convergence of heat flux by standing eddies for 1979–98. (a) Sep–Oct, (b) Nov–Dec, and (c) Jan–Feb. Contour specifications are the same as in Fig. 5.

aging the development of the standing eddies (e.g., Holopainen 1970). Geopotential height troughs form downstream of the Rockies and the Himalaya, with high-latitude extensions in eastern Canada and far eastern Siberia (Fig. 3b). The favored locations of the standing eddy features can be attributed to a combination of mid-latitude orography and land–sea distributions (e.g., Valdes and Hoskins 1989). The height and temperature trough axes are collocated over Canada, but are offset by about 30° longitude over eastern Siberia. Even though there is substantial local heating by the transient eddies and warm advection by the standing eddies, the Siberian cold air mass persists because of strong radiative cooling and lack of surface heating due to the region's isolation from the open oceans. The temperature trough is therefore a consequence of radiation and high-latitude land–sea–ice distributions while the height trough to its east is linked to midlatitude forcing. The offset between the mean temperature and height fields results in a contribution to the wintertime Arctic heat budget from the standing eddies that is especially important from eastern Siberia to the Bering Sea (Figs. 6b,c).

The changes in the mean flow at high latitudes from early to mid-winter are modest. The magnitude of the heating (and cooling) due to the transient and standing eddies increases, but the regional distribution is largely unchanged. The contrast between the eastern and western Arctic intensifies as tropospheric temperatures and geopotential heights continue to decrease over the Canadian Archipelago. Overland et al. (1997) state that this additional cooling in the western Arctic is caused by a tropospheric extension of the polar vortex and is maintained by radiative processes linked to upper-level temperature and humidity patterns. The results from the present study suggest that the development and maintenance of this feature may also be related to surface cooling over the Greenland plateau and its manifestation in the standing eddy heat fluxes.

The Arctic Oscillation

The 20-yr time period we have selected spans an important and unprecedented climate shift that occurred around 1989 in association with the Arctic oscillation (AO) (Thompson and Wallace 1998). The AO is characterized by latitudinal shifts of atmospheric mass that modulate the strength of the polar vortex. The spatial signature of the AO was noted earlier by van Loon and Williams (1980) who made a connection between sea level pressure in the North Atlantic–European area and the meridional component of the standing eddy heat flux in eastern Asia. Carleton (1988) and Rogers and Raphael (1992) also explored the effects of Northern Hemisphere teleconnection patterns on the meridional eddy heat fluxes. In light of these studies, we decided to explore the temporal variability of the eddy heat flux convergence in the context of the AO.

We wanted to know if the recent changes associated with the AO had an effect on the dynamics of the fall cooling cycle.

The monthly AO index values we use are the principal components of the leading EOF of sea level pressure poleward of 20°N based on all months starting in January 1958. The AO index values were derived by David Thompson using the NCEP reanalysis and are available online at http://tao.atmos.washington.edu/data/ao/. We compiled 2-month composites of the standing and transient eddy heat flux convergences for the positive and negative phases of the AO. The phases of the AO were evenly distributed in the fall and winter months over the 20-yr period so that each 2-month composite is based on roughly half of the total years. The AO was mostly negative in the 1980s and mostly positive in the 1990s. For each two-month period (September–October, November–December, and January–February) the differences between the AO-positive and AO-negative composite fields were tested for significance by comparing them to the sum of the standard errors of the composite means.

The results indicate that the general spatial patterns of the standing and transient eddy heat flux convergences were not significantly influenced by the changes associated with the AO. This may be because the dynamics of the AO are primarily stratospheric whereas the eddy heat fluxes are concentrated in the troposphere. A few small areas where the differences were significant were scattered around the Arctic in the fall and early winter, but these were mostly in locations where the eddy flux convergences were small. The notable exceptions occurred in midwinter, when the AO signature is strongest and the eddy flux convergences are at a maximum. We present the results for January–February in Fig. 7 to illustrate the regional influences of the AO. The top and middle panels of Fig. 7 show the two composite fields for the standing and transient eddy heat flux convergences; the bottom panels show the differences between them. The stippled areas in the bottom panels indicate where the differences are significant. The areas where the AO influences the transient eddy heat flux convergence are located south and east of Greenland, a region around the Icelandic low where the transient eddies play an important role in redistributing heat around the Arctic. For the standing eddy flux convergence, the regions significantly influenced by the AO are located east of Greenland, over Europe, and in east Asia. These results complement the analysis of Thompson and Wallace (2000), who identify other zonally varying structures in the AO. In a related study, Rogers and Thompson (1995) linked mild Siberian winters (a characteristic of the positive phase of the AO) to an increase in cyclone activity in the high-eastern Arctic. Thompson and Wallace (2000) speculated that transient eddy heat flux convergence contributed to this Siberian warming, but our results indicate that is not the case. In fact, the transient eddy heat flux convergence over Siberia is greater during the *negative* phase of the AO. Instead, the Siberian warming may be due to the radiative effects of the clouds and moisture that accompany the cyclones.

6. Summary

This paper has addressed the role played by transient and standing eddies in establishing regional temperature patterns in the Arctic throughout the fall cooling cycle.

At the end of summer, the mean flow is essentially zonally symmetric, but as the cold season progresses, the mean flow evolves into a wavenumber-2 pattern with colder temperatures and lower geopotential heights over northern Canada and Siberia and warmer temperatures and higher heights over the GIN Seas and over Alaska and the Chukchi Sea. There is a large net flux of heat and moisture into the Arctic atmosphere from the high-latitude oceans, but surface fluxes alone cannot account for the regional tropospheric temperature differences. That energy is redistributed horizontally around the Arctic by the eddy circulations. In the eastern Arctic, the transient eddies are especially important in transferring heat and moisture from the Barents and GIN Seas into the central Arctic. The standing eddies play the larger role in the heat budget on the Pacific side of the Arctic in early to mid-winter. The standing eddy flux convergence is especially large over eastern Siberia throughout the winter, and over northern Canada and Greenland during midwinter.

Eddy fluxes have been studied for the purpose of developing, verifying, and improving parameterizations for climate models (e.g., van Loon 1979; Genthon and Krinner 1998), but the advent of single-column modeling has made them important in a more direct way. The change in temperature due to horizontal energy transport is an essential requirement of single-column models (Bitz et al. 1996; Randall et al. 1996; Beesley and Moritz 1999; Pinto et al. 1999). A potential application of these results will be during the analysis and modeling phases of several recent Arctic field experiments (Randall et al. 1998). These projects involve column modeling and the integration of the point measurements into a larger framework that would be compatible with the large-scale coupled GCMs.

A comparison of the standing and transient eddy heat flux convergences during positive and negative phases of the AO indicated that the AO has a small significant effect on the flux parameters over the entire Arctic. However, on smaller spatial scales there are isolated regions (e.g., around the Icelandic low) where the AO does influence the Arctic heat budget. The regional variability of the dynamics and impacts of the AO will be a subject of our continuing research efforts.

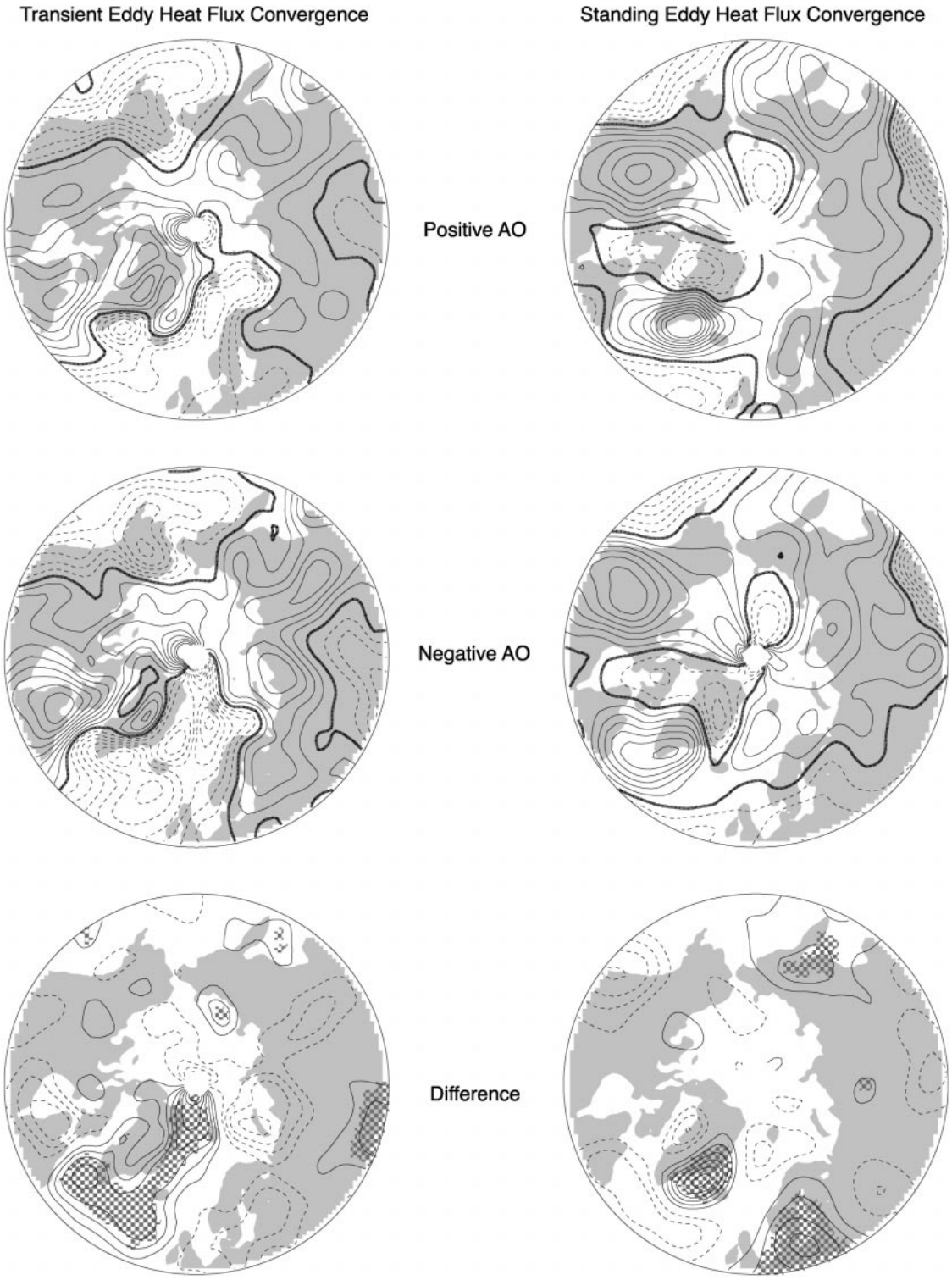

FIG. 7. The influence of the Arctic Oscillation (AO) on the standing and transient eddy heat flux convergences in midwinter (Jan–Feb). (Top panels) Positive-AO composites, (middle panels) negative-AO composites, and (bottom panels) differences; stippling indicates where the differences are significant. Contour interval for all plots is 25 W m^{-2}; no zero line is drawn in the difference plots.

Acknowledgments. This research was supported by NASA's Polar Research Program and the Arctic Program of the Office of Naval Research.

REFERENCES

Beesley, J. A., and R. E. Moritz, 1999: Toward an explanation of the annual cycle of cloudiness over the Arctic Ocean. *J. Climate,* **12,** 395–415.

Bitz, C. M., D. S. Battisti, R. E. Moritz, and J. A. Beesley, 1996: Low-frequency variability in the Arctic atmosphere, sea ice, and upper-ocean climate system. *J. Climate,* **9,** 394–408.

Carleton, A. M., 1988: Meridional transport of eddy sensible heat in winters marked by extremes of the North Atlantic Oscillation, 1948/49–1979/80. *J. Climate,* **1,** 212–223.

Genthon, C., and G. Krinner, 1998: Convergence and disposal of energy and moisture on the Antarctic polar cap from ECMWF reanalyses and forecasts. *J. Climate,* **11,** 1703–1716.

Gibson, J. K., P. Kållberg, S. Uppala, A. Hernandez, A. Nomura, and E. Serrano, 1997: ECMWF Reanalysis Project Report Series: 1. ERA description. ECMWF, 72 pp.

Hartmann, D. L., 1994: *Global Physical Climatology*. Academic Press, 411 pp.

Higuchi, K., C. A. Lin, A. Shabbar, and J. L. Knox, 1991: Interannual variability of the January tropospheric meridional sensible heat transport in the northern latitudes. *J. Meteor. Soc. Japan,* **69,** 459–472.

Holopainen, E., 1970: An observational study of the energy balance of the stationary disturbances in the atmosphere. *Quart. J. Roy. Meteor. Soc.,* **96,** 626–644.

——, and C. Fortelius, 1986: Accuracy of estimates of atmospheric large-scale energy flux divergence. *Mon. Wea. Rev.,* **114,** 1910–1921.

Hoskins, B. J., and R. P. Pearce, Eds., 1983: *Large-Scale Dynamical Processes in the Atmosphere.* Academic Press, 397 pp.

Kalnay, E., and Coauthors, 1996: The NCEP/NCAR 40-Year Reanalysis Project. *Bull. Amer. Meteor. Soc.,* **77,** 437–471.

——, R. Kistler, and M. Kanamitsu, 1998: NCEP/NCAR 40-Year Reanalysis overview. *Proc. First WCRP Int. Conf. on Reanalyses,* Silver Spring, MD, World Climate Research Programme, 1–7.

Kann, D. M., S.-K. Yank, and A. J. Miller, 1994: Mean meridional transport of energy in the earth–atmosphere system using NMC global analyses and ERBE radiation data. *Tellus,* **46A,** 553–565.

Keith, D. W., 1995: Meridional energy transport: Uncertainty in zonal means. *Tellus,* **47A,** 30–44.

Lau, N.-C., 1979: Observed structure of tropospheric stationary waves and the local balances of vorticity and heat. *J. Atmos. Sci.,* **36,** 996–1016.

Michaud, R., and J. Derome, 1991: On the mean meridional transport of energy in the atmosphere and oceans as derived from six years of ECMWF analyses. *Tellus,* **43A,** 1–14.

Mock, C. J., P. J. Bartlein, and P. M. Anderson, 1998: Atmospheric circulation patterns and spatial climatic variations in Beringia. *Int. J. Climatol.,* **10,** 1085–1104.

Nakamura, N., and A. H. Oort, 1988: Atmospheric heat budgets of the polar regions. *J. Geophys. Res.,* **93,** 9510–9524.

Overland, J. E., P. Turet, and A. H. Oort, 1996: Regional variation of moist static energy flux into the Arctic. *J. Climate,* **9,** 54–65.

——, J. M. Adams, and N. A. Bond, 1997: Regional variation of winter temperatures in the Arctic. *J. Climate,* **10,** 821–837.

Pinto, J. O., J. A. Curry, and A. H. Lynch, 1999: Modeling clouds and radiation for the November 1997 period of SHEBA using a column climate model. *J. Geophys. Res.,* **104,** 6661–6678.

Randall, D. A., K.-M. Xu, R. J. C. Somerville, and S. Iacobellis, 1996: Single-column models and cloud ensemble models as links between observations and climate models. *J. Climate,* **9,** 1683–1697.

——, and Coauthors, 1998: Status of and outlook for large-scale modeling of atmosphere–ice–ocean interactions in the Arctic. *Bull. Amer. Meteor. Soc.,* **79,** 197–219.

Rogers, J. C., and M. N. Raphael, 1992: Meridional eddy sensible heat fluxes in the extremes of the Pacific/North American teleconnection pattern. *J. Climate,* **5,** 127–139.

——, and E. M. Thompson, 1995: Atlantic Arctic cyclones and the mild siberian winters of the 1980s. *Geophys. Res. Lett.,* **22,** 799–802.

Schubert, S., R. B. Rood, and J. Pfaendtner, 1993: An assimilated dataset for earth science applications. *Bull. Amer. Meteor. Soc.,* **74,** 2331–2342.

Schweiger, A. J., and J. R. Key, 1994: Arctic Ocean radiative fluxes and cloud forcing estimated from the ISCCP C2 cloud dataset, 1983–1990. *J. Appl. Meteor.,* **33,** 948–963.

Serreze, M. C., J. E. Box, R. G. Barry, and J. E. Walsh, 1993: Characteristics of Arctic synoptic activity, 1952–1989. *Meteor. Atmos. Phys.,* **51,** 147–164.

——, J. R. Key, J. E. Box, J. A. Maslanik, and K. Steffen, 1998: A new monthly climatology of global radiation for the Arctic and comparisons with NCEP–NCAR reanalyses and ISCCP-C2 fields. *J. Climate,* **11,** 121–136.

Thompson, D. W. J., and J. M. Wallace, 1998: The Arctic Oscillation signature in the wintertime geopotential height and temperature fields. *Geophys. Res. Lett.,* **25,** 1297–1300.

——, and ——, 2000: Annular modes in the extratropical circulation. Part I: Month-to-month variability. *J. Climate,* **13,** 1000–1016.

Valdes, P. J., and B. J. Hoskins, 1989: Linear stationary wave simulations of the time-mean climatological flow. *J. Atmos. Sci.,* **46,** 2509–2527.

van Loon, H., 1979: The association between latitudinal temperature gradient and eddy transport. Part I: Transport of sensible heat in winter. *Mon. Wea. Rev.,* **107,** 525–534.

——, and J. Williams, 1980: The association between latitudinal temperature gradient and eddy transport. Part II: Relationships between sensible heat transport by stationary waves and wind, pressure, and temperature in winter. *Mon. Wea. Rev.,* **108,** 604–614.

Walsh, J. E., and W. L. Chapman, 1998: Arctic cloud–radiation–temperature associations in observational data and atmospheric reanalyses. *J. Climate,* **11,** 3030–3045.